

The Infancy of Cosmic Reionization

Rennan Barkana^{1,2,3*}

¹ *Institute for Cosmic Ray Research, University of Tokyo, Kashiwa 277-8582, Japan*

² *Division of Physics, Mathematics and Astronomy, California Institute of Technology, Mail Code 130-33, Pasadena, CA 91125, USA*

³ *Guggenheim Fellow; on sabbatical leave from the School of Physics and Astronomy, Tel Aviv University, Israel*

25 August 2021

ABSTRACT

We consider the early stages of cosmic hydrogen or helium reionization, when ionizing sources were still rare. We show that Poisson fluctuations in the galaxy distribution substantially affected the early bubble size distribution, although galaxy clustering was also an essential factor even at the earliest times. We find that even at high redshifts, a significant fraction of the ionized volume resided in bubbles containing multiple sources, regardless of the ionizing efficiency of sources or of the reionization redshift. In particular, for helium reionization by quasars, one-source bubbles last dominated (i.e., contained 90% of the ionized volume) at some redshift above $z = 7.3$, and hydrogen reionization by stars achieved this milestone at $z > 23$. For the early generations of atomic-cooling halos or molecular-hydrogen-cooling halos, one-source ionized regions dominated the ionized volume only at $z > 31$ and $z > 48$, respectively. To arrive at these results we develop a statistical model for the effect of density correlations and discrete sources on reionization and solve it with a Monte Carlo method.

Key words: galaxies:high-redshift – cosmology:theory – galaxies:formation

1 INTRODUCTION

The earliest generations of stars are thought to have transformed the universe from darkness to light and to have reionized and heated the intergalactic medium. Knowing how the reionization process happened is a primary goal of cosmologists, because this would tell us when the early stars formed and in what kinds of galaxies. The strong fluctuations in the number density of galaxies, driven by large-scale density fluctuations in the dark matter, imply that the dense regions reionize first, producing on large scales an inside-out reionization topology (Barkana & Loeb 2004). This basic picture has been studied and confirmed with detailed analytical models (Furlanetto et al. 2004), semi-numerical methods (Mesinger & Furlanetto 2007), and by a variety of large numerical simulations (Mellema et al. 2006; Zahn et al. 2007; Trac & Cen 2007) that solve gravity plus radiative transfer. The distribution of neutral hydrogen during reionization can in principle be measured from maps of 21-cm emission by neutral hydrogen (Madau et al. 1997), although upcoming experiments such as the Murchison Widefield Array (MWA)¹ and the Low Frequency Array (LOFAR)² are expected to be able to detect ionization fluctuations only

statistically (for reviews see, e.g., Furlanetto et al. 2006b; Barkana & Loeb 2007).

The infancy of cosmic reionization, when only a small fraction of the volume of the universe was ionized, is of interest for a number of reasons. First, when ionizing sources were rare at early times, they are expected to have formed separate H II bubbles which if observed can be used to study directly the properties of individual sources and their surroundings (Cen 2006), without the complications of later times, when overlapping bubbles imply that galaxy clustering dominates the ionization distribution and the 21-cm power spectrum. Second, when ionization fluctuations disappear over much of the universe, it becomes possible to use the 21-cm technique for other applications including those of fundamental cosmology, without the complications of ionization fluctuations which are intrinsically non-linear (since the ionization fraction varies from 0 to 1). Major such applications include measurements of the density power spectrum (Hogan & Rees 1979; Scott & Rees 1990), of fluctuations in the Ly α radiation emitted by the first galaxies (Barkana & Loeb 2005b; Pritchard & Furlanetto 2006; Chuzhoy, Alvarez & Shapiro 2006), and of fluctuations in the rate of heating from early X-rays (Pritchard & Furlanetto 2007). If ionization fluctuations are negligible then the angular anisotropy of the 21-cm power spectrum makes it possible to measure separately various fluctuation sources, including in particular the cosmologically-interesting baryonic density power spectrum

* E-mail: barkana@wise.tau.ac.il

¹ <http://www.haystack.mit.edu/ast/arrays/mwa/>

² <http://www.lofar.org/>

(Barkana & Loeb 2005a). On small scales, the existence of H II bubbles (even when rare) affects the fluctuations in Ly α and X-ray radiation, producing a small-scale cutoff in the 21-cm power spectrum that can be used to detect and study the population of galaxies that formed just 200 million years after the Big Bang (Naoz & Barkana 2008).

While analytical models and numerical simulations exist that can be used to study the later epochs of reionization, the early times are very difficult to investigate. Simulations, which in general must overcome the huge disparity between the large characteristic scales of galaxy clustering at high redshift and the small scales of individual galaxies (Barkana & Loeb 2004), are stretched even further at early times, when ionizing sources become very rare and even larger cosmological volumes are required in order to assemble a reasonable statistical sample. As discussed in detail below, current analytical models based on the model of Furlanetto et al. (2004) account for galaxy clustering but are based on continuous variables and cannot account for the fact that galaxies are discrete sources. This discreteness becomes a crucial factor in the early stages of reionization, when the number of ionizing sources per bubble is small. In this limit, Poisson fluctuations also become substantial, weakening the correlation between the galaxy distribution and the underlying large-scale density fluctuations in the dark matter. Discreteness can also play a significant role during the central stages of reionization, particularly in the case of He reionization by quasars, which are rare sources believed to form only in massive halos that correspond to many- σ density fluctuations at high redshift. These various aspects of discrete sources are not accounted for in current analytical models. Furlanetto & Oh (2008) considered helium reionization and showed that the continuous models break down when discreteness is important. They suggested to instead use a pure stochastic Poisson model, without halo correlations, when He is less than $\sim 50\%$ ionized globally.

In this paper we develop a model that accounts for discrete sources as well as density correlations. We solve the model with a Monte Carlo method and use it to show that galaxy correlations play a major role even in the infancy of cosmic reionization. Isolated one-source bubbles do dominate at sufficiently high redshifts, but the pure stochastic Poisson model is essentially never a good description of the bubble size distribution. In the next section we first review previous models (section 2.1), then develop ours (section 2.2) and summarize all the various models whose results we later compare (section 2.3). We illustrate our results during the infancy of reionization (section 3.1) and then develop an approximate calculation that allows us to scan through a wide parameter space of possible reionization scenarios (section 3.2). Finally, we illustrate our results during later stages of reionization (section 3.3) and summarize our conclusions (section 4). We assume a standard Λ CDM universe with cosmological parameters that match the five-year WMAP data and other large scale structure observations (Komatsu et al. 2008), namely $\Omega_m = 0.28$ (dark matter plus baryons), $\Omega_\Lambda = 0.72$ (cosmological constant), $\Omega_b = 0.046$ (baryons), $h = 0.7$ (Hubble constant), $n = 0.96$ (power spectrum index) and $\sigma_8 = 0.82$ (power spectrum normalization).

2 MODEL

Analytical approaches to galaxy formation and reionization are based on the mathematical problem of random walks with barriers. The statistics of a random walk with a barrier can be used to calculate various one-point distributions, including the distribution of ionized bubble sizes during reionization (Furlanetto et al. 2004). This distribution indicates how likely it is for each scale to determine whether a given point is ionized. As such, it indicates the relative importance of various scales in reionization, yielding important intuition about the internal dynamics of reionization. If bubbles of a given radius R are common, this produces a strong correlation in the neutral fraction (and thus 21-cm emission) on a scale $\sim R$, since the ionization states of two points separated by up to R are then often coupled. Calculations of the 21-cm correlation function using two-point extensions of the model yield reasonable agreement with numerical simulations (Furlanetto et al. 2004; Zahn et al. 2007; Barkana 2007) and indicate that the main feature of the power spectrum during reionization, i.e., enhanced large-scale power, indeed appears on scales corresponding to the most likely bubble sizes.

In this section we first review the basic setup of the random walk problem in the context of reionization. We then show how the standard approach can be generalized to solve for the bubble size distribution including Poisson fluctuations.

2.1 Reionization: basic setup

The basic approach for using random walks with barriers in cosmology follows Bond et al. (1991), who used it to rederive and extend the halo formation model of Press & Schechter (1974). In this approach we work with the linear overdensity field $\delta(\mathbf{x}, z) \equiv \rho(\mathbf{x}, z)/\bar{\rho}(z) - 1$, where \mathbf{x} is a comoving position in space, z is the cosmological redshift and $\bar{\rho}$ is the mean value of the mass density ρ . In the linear regime, the overdensity grows in proportion to the linear growth factor $D(z)$ (defined relative to $z = 0$), making it possible to extrapolate the initial density field at high redshift to the present by multiplication by the relative growth factor. Thus, in this paper the density δ and related quantities refer to their values linearly-extrapolated to the present. In each application there is in addition a barrier that signifies the critical value (as a function of scale) which the linearly-extrapolated δ must reach in order to achieve some physical milestone, which here corresponds to having a sufficient number of galaxies within some region in order to fully reionize it.

Considering an arbitrary point A in space (at a given z), we calculate as follows its probability of being inside H II bubbles of various sizes (Furlanetto et al. 2004). We consider the smoothed density around this point, first averaging over a large scale or, equivalently, including only small comoving wavenumbers k . We then average over smaller scales (i.e., include larger k) until we find the largest scale on which the averaged overdensity is higher than the barrier; in the application to reionization, we then assume that the point A belongs to an H II bubble of this size. Mathematically, if the initial density field is a Gaussian random field and the smoothing is done using sharp k -space filters, then the value

of the smoothed δ undergoes a random walk as the cutoff value of k is increased. Instead of using k , we adopt the (linearly-extrapolated) variance S of density fluctuations as the independent variable. While the solutions are derived in reference to sharp k -space smoothing, we follow the traditional extended Press-Schechter approach and substitute real-space quantities in the final formulas. In particular, S is calculated as the variance of the mass M enclosed in a spatial sphere of comoving radius r .

The appropriate barrier for reionization was derived by Furlanetto et al. (2004), who noted that the ionized fraction in a region is given by $x^i = \zeta F_{\text{coll}}$, where F_{coll} is the collapse fraction (i.e., the gas fraction in galactic halos) and ζ is the overall efficiency factor, which is the number of ionizing photons that escape from galactic halos per hydrogen atom (or ion) contained in these halos, divided by the number of times each hydrogen atom in the intergalactic medium must be reionized (where this number is assumed to be spatially uniform). In the extended Press-Schechter model (Bond et al. 1991), in a region containing a mass corresponding to variance S_R ,

$$F_{\text{coll}} = \text{erfc} \left(\frac{\delta_c(z) - \delta}{\sqrt{2(S_{\text{min}} - S_R)}} \right), \quad (1)$$

where S_{min} is the variance corresponding to the minimum mass M_{min} of a halo that hosts a galaxy, δ is the mean density fluctuation in the given region, and $\delta_c(z)$ is the critical density for halo collapse at z . In reality, the cosmic mean halo distribution in simulations is better described by the halo mass function of Sheth & Tormen (1999) (with the updated parameters suggested by Sheth & Tormen (2002)). However, an exact analytical generalization is not known for the biased F_{coll} in regions of various sizes (corresponding to S_R) and mean density fluctuations δ .

Barkana & Loeb (2004) suggested a hybrid prescription that adjusts the abundance in various regions based on the extended Press-Schechter formula (Bond et al. 1991), and showed that it fits a broad range of simulation results. In general, we denote by $f(\delta_c(z), S) dS$ the mass fraction contained at z within halos with mass in the range corresponding to variance S to $S+dS$, where $\delta_c(z)$ is the critical density for halo collapse at z . Then the biased mass function in a region of size R (corresponding to density variance S_R) and mean density fluctuation δ is (Barkana & Loeb 2004)

$$f_{\text{bias}}(\delta_c(z), \delta, S_R, S) = \frac{f_{\text{ST}}(\delta_c(z), S)}{f_{\text{PS}}(\delta_c(z), S)} f_{\text{PS}}(\delta_c(z) - \delta, S - S_R), \quad (2)$$

where f_{PS} and f_{ST} are, respectively, the Press-Schechter and Sheth-Tormen halo mass functions. The value of $F_{\text{coll}}(\delta_c(z), \delta, S_R, S)$ is the integral of f_{bias} over S , from 0 up to the value S_{min} that corresponds to the minimum halo mass M_{min} or circular velocity $V_c = \sqrt{GM_{\text{min}}/R_{\text{vir}}}$ (where R_{vir} is the virial radius of a halo of mass M_{min} at z). We then numerically find the value of δ that gives $\zeta F_{\text{coll}} = 1$ at each S_R , yielding the exact barrier. Also, in order to compare with a simpler, analytically-solvable model, we derive a linear approximation to the barrier, $\delta(S_R) \approx \nu + \mu S_R$, by numerically finding the value of the barrier at $S_R = 0$ and its derivative with respect to S_R . In general, photon conservation implies that the mean global ionized fraction

should equal $\bar{x}^i = \zeta \bar{f}_{\text{ST}}$ in terms of the cosmic mean collapse fraction.

Barkana (2007) and Barkana & Loeb (2008) used an approximation in which effectively each factor on the right-hand side of equation (2) was integrated separately over S , yielding a simple analytical formula for the effective linear barrier. This approximation was also assumed by Furlanetto et al. (2006a) when they stated that this hybrid prescription does not change the bubble size distribution from the pure Press-Schechter case (for a fixed redshift, minimum halo mass, and cosmic mean ionized fraction). Here we solve numerically for the barrier using the exact formulas. We show that the previously-used approximation is not too accurate, especially at the early stages of reionization that are our focus in this paper.

2.2 The statistics of a random walk with a barrier and discrete sources

The standard approach presented above treats the random walks as functions of a continuous variable S_R , and assumes a one-to-one correspondence between the value of δ and the ionized fraction x^i at each scale. The statistical distribution of first barrier crossing, which physically corresponds to the bubble size distribution, can be derived analytically for the approximate linear barrier (Furlanetto et al. 2004), and for the exact barrier can be solved with Monte Carlo simulations of random walks or by solving an integral equation (Zhang & Hui 2006).

In reality, there are two additional physical constraints that are neglected in the standard approach: the ionizing sources are discrete, and the ionized fraction (for a given value of δ in a region) fluctuates due to Poisson fluctuations in the number of galaxies. The discreteness of ionizing sources means that the possible volume of bubbles has a minimum value V_{bub} corresponding to the bubble due to a single galaxy hosted by a halo of mass M_{min} . Also, the expected ionized fraction x^i given by the continuous model is subject to Poisson fluctuations, as the actual ionized fraction depends on the number of galaxies. Unlike the standard random walk approach, in which the statistics of the walk depend only on the barrier expressed as a function $\delta(S_R)$, Poisson fluctuations introduce an explicit dependence on the mapping between S_R and scale R .

In order to include these discrete aspects in the bubble distribution, we begin with the standard analytical approach, which considers the statistics of spherical volumes of various sizes R , all about a point A . Given a value δ on a scale R (with corresponding variance S_R), we now treat the continuous ionized fraction x^i of the previous subsection only as an average expectation value. To find its real distribution, we first calculate the mean expected value $\langle j \rangle$ of the number of ionizing sources within the sphere of radius R . This (non-integer) value can be calculated from the integral of $f_{\text{bias}} dS$ weighted by $1/M$ (which yields halos weighted by number rather than mass); it depends on z , S_{min} , δ , and S_R . The actual value of j is given by a Poisson distribution with mean equal to $\langle j \rangle$. To find the actual x^i , we find the mass of each of the j halos according to the halo mass distribution given by f_{bias} ; note that this procedure does not involve a single, fixed mass distribution since f_{bias} is a function of δ and S_R .

The complicating factor in this procedure is that we cannot treat each scale R independently, since the ionizing sources are correlated among the various volumes. This is the case first because the densities δ are correlated, and second because the Poisson fluctuations are correlated, since each sphere contains all the galaxies that lie within all smaller enclosed spheres. The correlation of the densities is dealt with in the standard way reviewed above, where small-scale power is added gradually as smaller spheres are considered. This makes $\delta(S_2)$ dependent on $\delta(S_1)$ if $S_2 > S_1$, forcing us to start on large scales $S_R = 0$ and go to smaller ones. However, the Poisson fluctuations are correlated in the other direction, since a region S_2 contains a region S_1 if $S_2 < S_1$.

The solution is a two-step Monte Carlo method: first, we generate the random walk $\delta(S_R)$, going from $S_R = 0$ to its maximum value (corresponding to the minimum bubble volume V_{bub}) in equal steps. At each S_R step, we find the mean expected number of galactic halos $\langle j \rangle(S_R)$ and the mean expected total mass of these halos, $\langle M_{\text{tot}} \rangle(S_R)$. Note that the mean expected ionized fraction is $\langle x^i \rangle(S_R) = \zeta \langle M_{\text{tot}} \rangle(S_R) / M(S_R)$, where $M(S_R)$ is the total mass contained within the spherical volume of radius R . In the second step, we generate the actual ionized fractions starting from the smallest scale, V_{bub} , and working outwards. At V_{bub} , we generate an instance of a Poisson distribution with mean $\langle j \rangle(S_R)$, yielding an actual integer number j of halos, for each of which we find its mass from the appropriate distribution of halo number versus mass, derived from f_{bias} . Then, for each larger scale (i.e., smaller S_R value), the additional number of galaxies from the last step is on average expected to be the difference $\langle \Delta j \rangle = \langle j \rangle(S_1) - \langle j \rangle(S_2)$, where $S_1 < S_2$ are two consecutive steps in S_R . We find the actual difference Δj from a Poisson distribution with a mean of $\langle \Delta j \rangle$. However, while an actual number of galaxies cannot be negative, sometimes the random walk in δ gives a value $\langle \Delta j \rangle < 0$. In this case we assume that $\Delta j = 0$, since the number of galaxies already enclosed in a smaller volume (corresponding to S_2) must also be found in the larger, enclosing volume (S_1). We do not discard the negative value of $\langle \Delta j \rangle$ but add it in the next step to the next value of $\langle \Delta j \rangle$, continuing until we reach a positive expected mean value on which we can operate a Poisson distribution. In each step, we also keep track of the expected total mass difference, $\langle \Delta M \rangle = \langle M_{\text{tot}} \rangle(S_1) - \langle M_{\text{tot}} \rangle(S_2)$. We slightly modify³ each distribution f_{bias} that we use to generate the individual halo masses so as to give the correct expected $\langle \Delta M \rangle$. This procedure ensures that on each scale we obtain the correct average number of galaxies and correct average galaxy mass, both to high accuracy. We note also that in each step in S_R , even if δ at the end of the step is below the barrier, there is a chance that the random walk hit the barrier during the step. We estimate this probability using a linear barrier approximation applied separately to each step, and if the walk hit the barrier then we raise δ at the end of the step to the barrier. This procedure greatly accelerates the convergence of the

results as a function of the total number of steps adopted in S_R .

2.3 Summary of models

We summarize here the various models for the bubble size distribution that we consider and compare below.

(i) Model A: The correct distribution as given by our full model. The bubble size distribution is calculated with our Monte Carlo method with discrete sources and Poisson fluctuations, as detailed in section 2.2. We also keep track of how many sources are contained in each generated bubble, which allows us to find the cumulative volume fraction contained in bubbles with at least N sources, as a function of N .

(ii) Model B: The exact, continuous barrier (without Poisson fluctuations or discreteness). We calculate the non-linear barrier $\delta(S_R)$ numerically, as detailed in section 2.1. We then derive the bubble size distribution with a Monte Carlo method that generates random walks and tracks where they first cross the barrier.

(iii) Model C: A continuous linear barrier approximation. We calculate a linear barrier approximation $\delta(S_R) \approx \nu + \mu S_R$ numerically, as detailed in section 2.1. We then derive the bubble size distribution analytically as in Furlanetto et al. (2004).

(iv) Model D: The previously-used continuous linear barrier approximation. Here we apply the additional approximation mentioned at the end of section 2.1, where we noted that it gives the same bubble size distribution as in the linear barrier approximation of the pure Press-Schechter (rather than Sheth-Tormen) model. In this case we calculate analytically a linear barrier approximation $\delta(S_R) \approx \nu + \mu S_R$ and then derive the resulting bubble size distribution analytically as in Furlanetto et al. (2004).

(v) Model E: The pure stochastic Poisson model suggested by Furlanetto & Oh (2008). This model, which neglects halo correlations and assumes randomly placed, equal-intensity sources, yields an analytical result (Furlanetto & Oh 2008) for the cumulative volume fraction contained in bubbles with at least N sources.

Note that the minimum bubble scale is V_{bub} for models A and E, and V_{bub}/ζ (corresponding to the scale of the minimum halo mass M_{min}) for models B–D. Also note that we have tested our barrier-crossing Monte-Carlo code by comparing it to the analytical solution of a continuous linear barrier (Models C and D). We have confirmed precise convergence, to within a relative error below 1% in the total ionization probability, i.e., the total probability of crossing the barrier.

3 RESULTS

We illustrate our results for a wide range of possible parameters for either hydrogen reionization or helium (full) reionization. In the latter case, ζ is simply interpreted as the overall efficiency factor of producing helium-ionizing photons in halos. For hydrogen, minimum halo masses M_{min} that are often considered are the minimum mass for atomic cooling (corresponding to a circular velocity $V_c \sim 16.5$ km/s, where

³ We scale the input M value of the cumulative distribution of halo mass M (so that the total probability of having $M \geq 0$ remains unity), with the scaling factor (typically close to unity) chosen to yield the correct mean halo mass.

$V_c = \sqrt{GM/R}$ in terms of the halo virial mass and radius), or (at very high redshift) the minimum mass for molecular hydrogen cooling ($V_c \sim 4.5$ km/s). Also, much larger minimum masses are possible, $V_c \sim 35$ km/s due to photoionization feedback (which should affect most of the universe by the time reionization is well advanced), or even larger values if internal supernova feedback strongly decreases the star formation efficiency of low-mass halos at high redshift. For helium reionization, assuming it occurs much later, photoionization feedback affects the source halos from an early stage when the density of the assembling matter is still low, resulting in a larger $V_c \sim 80$ km/s (i.e., of order the Jeans mass). Furthermore, if the observed super-linear local relation between halo and black hole mass holds at high redshift, then quasars are relatively much brighter in more massive halos, increasing the typical halos of helium-ionizing sources to $V_c \sim 200 - 300$ km/s. For a given V_c , the efficiency ζ can be chosen to give complete reionization⁴ $\bar{x}^i = 1$ at various redshifts z_{rei} . For a fixed z_{rei} , a larger M_{min} implies that rarer halos caused reionization, resulting in larger Poisson fluctuations.

3.1 Basic results and comparison with previous models

We begin by considering examples corresponding to an early stage (mean ionized fraction $\bar{x}^i = 1\%$) of hydrogen or helium reionization. For hydrogen, we assume atomic cooling ($V_c = 16.5$ km/s), with efficiency set to complete reionization (i.e., $\bar{x}^i = 1$) at $z_{\text{rei}} = 7$ (implying $\zeta = 19$). For helium we assume $z_{\text{rei}} = 3$ and $V_c = 285$ km/s (implying $\zeta = 95$), which gives the bubbles a minimum size at $z \sim 3$ of $R = 10$ Mpc, about the expected size for the quasars that are observed to dominate the ionizing photon production at that redshift (Furlanetto & Oh 2008). Figure 1 shows that the bubble size distribution obtained from our full model is substantially different from the predictions of previous models that are based either on a continuous barrier or on a purely stochastic Poisson distribution.

In general these models, based as they are on spherical statistics, do not precisely conserve photons, and thus do not yield precisely the desired $\bar{x}^i \equiv \zeta \bar{f}_{\text{ST}}$ which we have set to 1%. Indeed, the raw total ionization probability yielded by the models is 2.1% (H) and 2.0% (He) for model D, 0.90% (H) and 1.4% (He) for model C, and 1.3% (H) and 1.4% (He) for model A. Thus, in the figure we compare the relative distributions, expressed in terms of the fraction F_i of the ionized volume contained in various bubbles. Note that model E is defined according to the desired \bar{x}^i , and model B (the exact continuous barrier) is mathematically consistent in the sense that it yields the correct total \bar{x}^i if the probability is integrated down to $V = V_{\text{bub}}/\zeta$ (We have numerically verified this mathematical consistency to a relative error of $\sim 1\%$).

Discreteness strongly fails for the continuous barrier

⁴ Note that our simple model does not include the likely added importance of recombinations towards the end of reionization. However, in this paper we do not consider the late stages of reionization except as a convenient fiducial mark for normalizing ζ through z_{rei} .

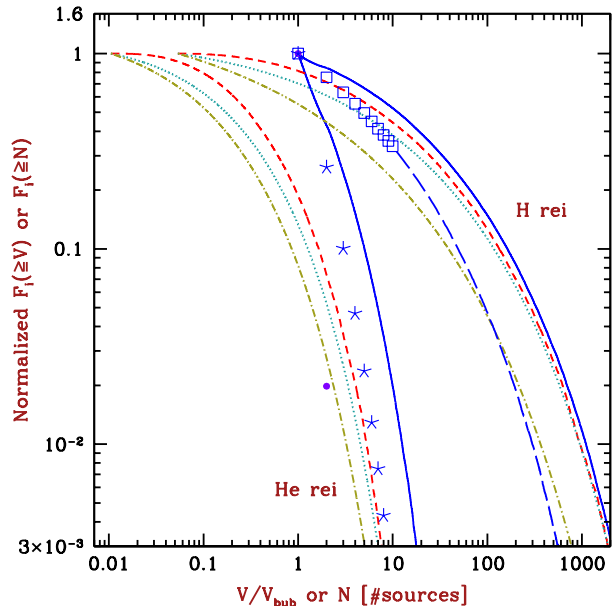


Figure 1. Cumulative bubble volume distribution as a function of V/V_{bub} , or of the number N of ionizing sources in the bubble. Assuming $z_{\text{rei}} = 7$ and $V_c = 16.5$ km/s for H, and $z_{\text{rei}} = 3$ and $V_c = 285$ km/s for He, we consider $\bar{x}^i = 1\%$ ($z = 16.3$ for H, 6.3 for He). We compare $F_i(\geq V)$, the fraction of the ionized volume contained in bubbles with volume $\geq V$, from our full Monte Carlo method with discrete sources (Model A; solid curves) to $F_i(\geq V)$ from a continuous barrier (Model B; short-dashed curves), a continuous linear barrier approximation (Model C; dotted curves), and a continuous linear Press-Schechter barrier (Model D; dot-dashed curves). We also show $F_i(\geq N)$, the fraction of the ionized volume contained in bubbles containing $\geq N$ sources, from our full model (Model A; H: squares, He: stars; long-dashed curves for $N > 10$), and from a pure Poisson model (Model E; circles).

models (both linear and non-linear), in the sense that much of the ionized volume in these models is predicted to occur inside bubbles below the minimum volume V_{bub} , especially in the case of Helium reionization. Indeed, $F_i(\geq V_{\text{bub}})$ is only 55% (H) and 8.2% (He) for model D, 70% (H) and 13% (He) for model C, and 82% (H) and 19% (He) for model B. Thus, the continuous barrier models fail since they assign a substantial probability to the unphysical case of fractional bubbles that are produced by less than one source. Expressed differently, the continuous barrier models underpredict $F_i(\geq V_{\text{bub}})$ since they do not include the Poisson fluctuations that allow large regions to sometimes reach $x^i = 1$ even when their mean expected ionized fraction $\langle x^i \rangle (S_R)$ is below unity.

Figure 1 also illustrates the continuous model with a linearly approximated barrier, a model used very commonly because it yields analytical predictions (Furlanetto et al. 2004). The error of the linear barrier approximation grows at small scales, and becomes a 10% error in the barrier height at $V \sim 0.07V_{\text{bub}}$ (H) or $V \sim 0.02V_{\text{bub}}$ (He). However, the linear barrier approximation becomes relatively accurate on scales larger than the scale V_{bub} corresponding to a one-source bubble. On that scale, the height of the linear barrier in the examples shown here is only slightly below the height of the real barrier (by 2.6% for H and just 0.05% for He),

though when $\bar{x}^i \ll 1$ the barrier corresponds to a rare $\sim 3\text{-}\sigma$ fluctuation on this scale (and rarer still at larger scales), and thus small differences in barrier height translate to larger differences in F_i . The figure also shows that the pure Press-Schechter model (model D) is a rather poor approximation to model C. The Sheth-Tormen hybrid model yields more large bubbles than the Press-Schechter model, which agrees with the expectation based on the Sheth-Tormen mean halo mass function, which yields more rare, massive halos than does the Press-Schechter mass function.

While the continuous barrier model extends unphysically to $V < V_{\text{bub}}$, it does indicate correctly the fact that $F_i(\geq V)$ declines much more rapidly with V for the He case we consider than for H reionization. In fact, we find that if we simply cut off the $V < V_{\text{bub}}$ portion and renormalize the continuous models relative to $V = V_{\text{bub}}$ (which is not a standard way of interpreting these models), then the exact and linear barrier models yield nearly identical results, and they both yield a reasonable rough estimate to the true bubble size distribution in the full model. This is illustrated in Figure 2, which shows the same quantities as in Figure 1 except that all the continuous models have been renormalized and are plotted only for $V \geq V_{\text{bub}}$. For instance, the ratio $V_{1/2} \equiv F_i(V \geq V_{\text{bub}})/F_i(V \geq 2V_{\text{bub}})$ is 1.18 (H) and 2.33 (He) in the full model (model A), 1.14 (H) and 2.54 (He) for the continuous exact barrier (model B), and 1.15 (H) and 2.58 (He) for the continuous linear barrier (model C). This approach to the continuous models provides a reasonable estimate of the full bubble size distribution in the case of H reionization; e.g., $V_{1/100} \equiv F_i(V \geq V_{\text{bub}})/F_i(V \geq 100V_{\text{bub}})$ for H is 6.73 in model A, 6.46 in model B, and 6.21 in model C, so that here the linear model C, calculated analytically (i.e., without using Monte Carlo random walks or Poisson fluctuations), yields an estimate of $V_{1/100}$ that is within 8% of the true answer according to model A. However, for He reionization this approach is much less successful in predicting ratios involving large volumes; e.g., $V_{1/5} \equiv F_i(V \geq V_{\text{bub}})/F_i(V \geq 5V_{\text{bub}})$ for He is 9.9 in model A, 16.0 in model B, and 17.6 in model C, and these differences increase with V (Figure 2).

With our full model (model A), we can also separately predict the distribution by number $F_i(\geq N)$. This drops more rapidly with N than the distribution by volume $F_i(\geq V)$ does with V , since large-volume bubbles can be produced either by having many sources of mass $\sim M_{\text{min}}$ or with a smaller number of individually massive halos taken from the high-mass end of the halo mass function. Still, $F_i(\geq N)$ declines with N much more slowly than a pure Poisson model would predict. Indeed, a purely stochastic model as suggested by Furlanetto & Oh (2008) for the early stages of He ionization (or even as late as $\bar{x}^i \sim 50\%$), where Poisson fluctuations are assumed that are uncorrelated with the underlying density distribution, completely fails to describe the results. The analytical predictions of this model (Furlanetto & Oh 2008) yield, for $\bar{x}^i = 1\%$ (for either H or He), $F_i(N \geq 2) = 2.0 \times 10^{-2}$ and $F_i(N \geq 3) = 4.4 \times 10^{-4}$ (with the latter already outside the range of Figures 1 and 2). In particular, the ratio from the previous paragraph (but applied to the number of sources), $N_{1/2} \equiv F_i(N \geq 1)/F_i(N \geq 2)$, is 1.32 (H) or 3.8 (He) in the full model, compared to $N_{1/2} = 51$ for model E. Clearly, density correlations play a substantial role in deter-

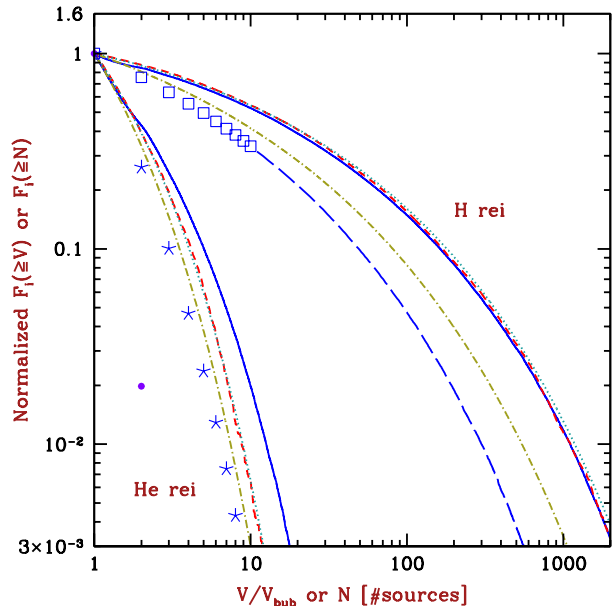


Figure 2. Cumulative bubble volume distribution as a function of V/V_{bub} , or of the number N of ionizing sources in the bubble. Same as Figure 1, except that the continuous models (models B–D) have been cut off below $V = V_{\text{bub}}$ and renormalized at that point. Note that the curves for models B and C nearly overlap.

mining the abundance of multi-source bubbles, even early on in reionization and even when the process is driven by large, rare ionizing sources (such as quasars).

To help understand the relation of the full model to the pure Poisson and to the continuous barrier models, we show in Figure 3 the relation between ionization in bubbles and the underlying linear density δ . Density fluctuations are strongly correlated with ionization, so that the density of ionized regions is strongly biased high, and the distribution is very different from the standard Gaussian that would be expected in a pure Poisson model. However, Poisson fluctuations allow regions to fully ionize themselves even if their density is significantly lower than the barrier, which in a continuous model would set the minimum needed δ for ionization by internal sources. In particular, the median δ for regions ionized by exactly N sources (where ‘exactly’ means not contained in any larger H II region) represents a fluctuation of $2.4\text{-}\sigma$, $2.57\text{-}\sigma$, and $2.61\text{-}\sigma$ (for H) or $1.9\text{-}\sigma$, $2.4\text{-}\sigma$, and $2.7\text{-}\sigma$ (for He), for $N = 1, 2$, and 3 , respectively. The corresponding (median) barriers, on the other hand, are $2.907\text{-}\sigma$, $2.909\text{-}\sigma$, and $2.922\text{-}\sigma$ (for H), or $3.2\text{-}\sigma$, $3.5\text{-}\sigma$, and $3.7\text{-}\sigma$ (for He). Thus, the barriers do give a good rough indication in each case of whether the δ distributions for various N are spaced out or squeezed together. This in turn determines whether one-source bubbles are dominant and $N > 1$ is rare, or if multi-source bubbles are at least as common as $N = 1$.

The continuous model indicates that the main parameters controlling the relative dominance of single-source bubbles are the effective efficiency ζ and the effective slope of the power spectrum on the scale R_{bub} of a one-source bubble. The efficiency sets the ratio between the scale R_{bub} of a one-source bubble and the scale R_{min} from which a galactic

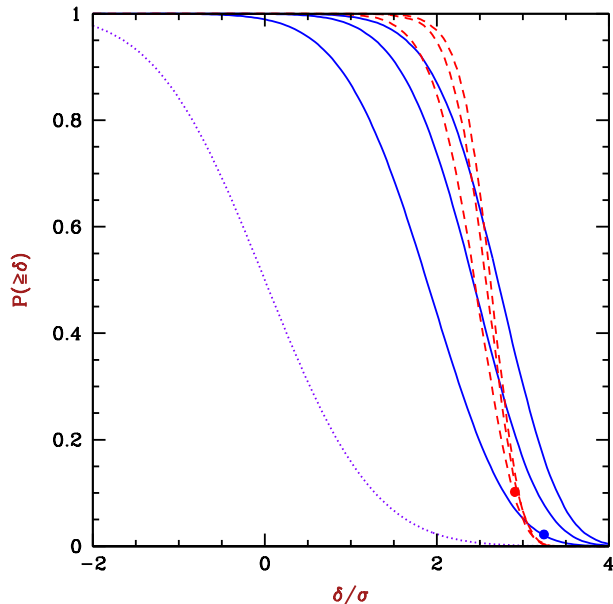


Figure 3. Cumulative probability distribution of the linear density δ in units of its standard deviation $\sigma = \sqrt{S}$ on the relevant scale. For either H (dashed curves) or He (solid curves) reionization with the same parameters as in Figure 1, we show $P(\geq \delta)$ for regions ionized by exactly one, two, or three sources (from left to right in each set of curves). In each case, a circle on the one-bubble curve shows the median barrier height on the corresponding scale. Also shown for comparison is the cumulative distribution of the normal distribution for unconstrained regions (dotted curve).

halo of mass M_{\min} was assembled (this ratio equals $\zeta^{1/3}$). Now, the key issue is the relative difficulty of each scale achieving self-ionization, when we consider different scales. To self-ionize, a region must reach a high enough collapse fraction, which according to the extended Press-Schechter formula in equation (1), requires a value of δ that depends on the variance ($S_{\min} - S_R$) available for density fluctuations inside the region⁵. In order to reach this required value (i.e., the barrier), the density has the variance S_R to work with. Thus, when we increase the scale (e.g., going from a typical one-source bubble to one with two sources), if the fractional decline in S_R is more rapid than in ($S_{\min} - S_R$), then self-ionized regions become rarer quickly with increasing scale, leading to the dominance of one-source bubbles. This is the case when $S_R \ll S_{\min}$, i.e., it requires first that the bubble and halo scales differ by a large factor (which requires large values of ζ), and also that the variance depend significantly on scale (otherwise, S_R and S_{\min} will be about the same even if the corresponding scales are very different).

More quantitatively, the fractional decline in S_R , over the fractional decline in ($S_{\min} - S_R$), is (for small changes in S_R) equal to $(S_{\min}/S_R - 1)$. If the power spectrum of density fluctuations is approximated as a power law with an effective index n over the relevant range of scales, then this ratio, which indicates how much harder (in terms of number

of σ of the fluctuation) it is to ionize larger scales, is approximately $\zeta^{1+(n/3)} - 1$. On small scales, n approaches the asymptotic value of -3 , making all scales behave roughly equally even when ζ is relatively large. Note, though, that increasing ζ increases R_{bub} and thus brings larger scales into play, making the effective n less negative and thus boosting the effect of the increased ζ on making few-source bubbles dominant. This puts a quantitative face on the intuition that rare sources tend to create bubbles with small numbers of sources. To illustrate, in our H example $R_{\min} = 64$ kpc and $R_{\text{bub}} = 169$ kpc, giving $n \sim -2.5$, while in the He example $R_{\min} = 1.7$ Mpc and $R_{\text{bub}} = 7.8$ Mpc, giving $n \sim -2$. Thus, He reionization by quasars has both a high efficiency and corresponds to a relatively large scale, both of which contribute to making small bubbles more dominant, in particular the smallest bubbles created by single sources.

3.2 Approximate calculation

The current lack of observations at high redshifts leaves basic parameters of the galaxy population unconstrained at early times. While our model can be used to calculate the bubble distribution in any particular case, the need to run Monte Carlo trials makes it difficult to explore a large parameter space. Thus, an approximate but quick calculation is useful for this purpose. In developing such an approximation, we focus on determining when one-source bubbles dominate the ionizing volume. This can be investigated with the ratio $N_{1/2}$, which is close to unity when multi-source bubbles dominate, and is $\gg 1$ when one-source bubbles do. Specifically, this ratio is related to the fraction $F_i(N = 1)$ of the ionized volume that is contained in one-source bubbles through $N_{1/2} = 1/[1 - F_i(N = 1)]$.

To construct an approximate calculation of this ratio we first adopt the approximation of having equal intensity sources, all corresponding to halos having a mass equal to the mean expected mass ($\langle M \rangle$). While this approximation does not work well for obtaining information on the bubble size distribution, we find that it works reasonably for our desired ratio involving the distribution of number of sources per bubble. We first consider in general the self-ionization probability on the scale of a bubble containing j sources (with a variance S that we approximate as that corresponding to a volume jV_{bub}), i.e., the probability that a region of this size contains at least j sources (regardless of whether or not it is contained in some larger bubble). A first attempt to calculate this quantity $P_{\text{self}}(j)$ is to calculate the Poisson probability of having at least j sources, averaged over the normal distribution of δ on the scale S :

$$P_{\text{self}}(j) = \int d\delta \frac{1}{\sqrt{2\pi S}} e^{-\delta^2/(2S)} P_{\text{Pois}}(j\tilde{x}^i(\delta, S); \geq j), \quad (3)$$

where $P_{\text{Pois}}(\alpha; \geq j)$ denotes the probability of having at least j sources in a Poisson distribution with mean α , and \tilde{x}^i (which also depends on z and S_{\min}) is an approximate estimate of $\langle x^i \rangle$ where we use the same approximation as in model D in order to obtain a simple formula. For large bubbles, equation 3 for $P_{\text{self}}(j)$ underestimates the self-ionization probability, since for a given mean δ in the region, internal density fluctuations increase the variance of the number of sources beyond a pure Poisson distribution. For $j = 2$ we can instead calculate a more accurate self-

⁵ The Sheth-Tormen hybrid model alters things slightly, but we use the simpler formula here as a rough guide for a qualitative understanding.

ionization probability by calculating a double integral over the joint normal distribution of δ_1 and δ_2 , the mean densities inside a one-source volume V_{bub} and inside the surrounding two-source volume, respectively. Given δ_1 and δ_2 , the mean expected number of sources in the two regions is $n_1 = \bar{x}^i(z, S_{\text{min}}, \delta_1, S_1)$ and $n_2 = 2\bar{x}^i(z, S_{\text{min}}, \delta_2, S_2)$, respectively, where S_1 and S_2 are the corresponding variances. The probability of self-ionization of the two-source volume is then the probability of having at least 2 total sources from the sum of a Poisson distribution of mean n_1 plus a Poisson distribution of mean $n_2 - n_1$ (except that the latter quantity is restricted to be non-negative, a key point which allows the larger fluctuations in n_1 to contribute).

Calculating $P_{\text{self}}(j)$ exactly for $j > 2$ would require at least a triple integration, but since $j = 1$ and $j = 2$ are most important for estimating $N_{1/2}$, we simply estimate the self-ionization probability for all $j > 2$ with equation (3). Now, $P_{\text{self}}(j)$ for any j is itself only a lower limit for the ionization probability $P(N \geq j)$, since the region may be part of a larger H II bubble even if it cannot fully ionize on its own. Actually, when one-source bubbles dominate and $P(N \geq j)$ drops rapidly with j , regions are much more likely to self-ionize than to get ionization help from larger scales, and then $P_{\text{self}}(j)$ becomes an accurate estimate of $P(N \geq j)$. However, in order to achieve reasonable accuracy also when multi-source bubbles are important, we add a correction to each $P_{\text{self}}(j)$ based on the values of $P_{\text{self}}(k)$ for $k > j$. Indeed, instead of just calculating $P_{\text{self}}(k)$, which is the probability of having at least k sources in a region of size corresponding to k sources, we can separately estimate $P_l(k)$, the probability of having exactly l sources in that region, using a formula just like equation (3) but using the Poisson probability of finding l sources. Then, for any number $l \geq k$ sources, we calculate the additional ionization probability that was not previously included in $P(N \geq j)$ (for each internal volume $j < k$) using the approximation that the l sources are uniformly distributed within the volume k . In this way, we estimate the probabilities $P(N \geq 1)$ and $P(N \geq 2)$ including the contributions of larger volumes with $j > 2$. When one-source bubbles dominate, higher- j volumes have a small effect, but when multi-source bubbles dominate the effect adds up, and we cut off j so that $P(N \geq 1)$ does not rise above the global ionization fraction \bar{x}^i . Actually, we find that while the correction from higher- j volumes can change each of $P(N \geq 1)$ and $P(N \geq 2)$ by up to a factor of a few (giving results much closer to the full model A), the relative effect on their ratio is $\sim 15\%$ at most.

Our estimate for $N_{1/2}$ is simply $P(N \geq 1)/P(N \geq 2)$. The approximate calculation becomes exact in the limit $N_{1/2} \rightarrow \infty$, where our estimated probabilities $P_{\text{self}}(j)$ become very small for all $j \geq 2$, while in the opposite limit, when $N_{1/2} \rightarrow 1$ all quantities become nearly independent of j and thus our estimate for the ratio approaches unity, also correctly. In practice, from direct comparison with the Monte Carlo method at \bar{x}^i ranging from 10^{-6} to 1, and at ratios $N_{1/2}$ ranging from 1 to 200, we find that our approximation for this ratio is accurate to $\sim 15\%$ (though below we extrapolate it beyond the tested range).

Having developed a quick, relatively accurate calculation method, we can use it to explore which areas of parameter space will be dominated by one-source bubbles and which will form many multi-source bubbles. Figures 4 and

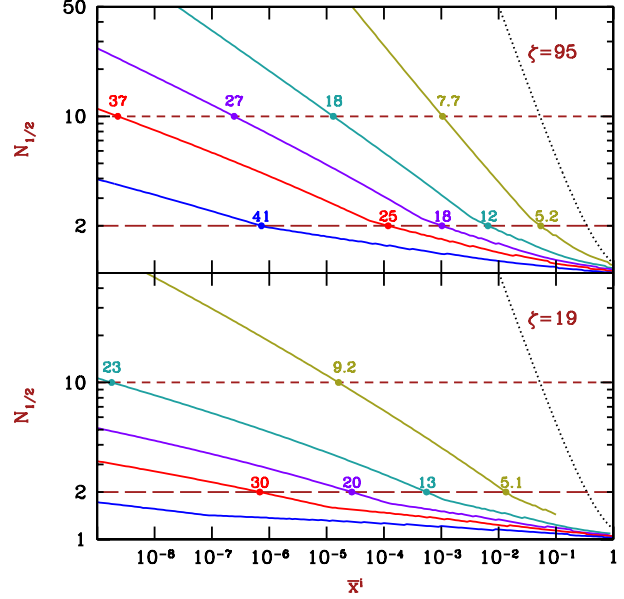


Figure 4. Sweep of the parameter space using our approximate calculation, showing the relative dominance of one-source compared to many-source bubbles as indicated by the ratio $N_{1/2} = P(N \geq 1)/P(N \geq 2)$. For $\zeta = 19$ or 95 , as indicated, we consider galactic halos with minimum $V_c = 4.5, 16.5, 35, 80,$ or 285 km/s (solid curves, from bottom to top). We compare to the case of a pure stochastic Poisson distribution (model E; dotted curves). Also shown are the locations corresponding to half of the volume being in one-source bubbles (horizontal long-dashed line), and to 90% in one-source bubbles (horizontal short-dashed line); redshifts are indicated at these locations for each case (if it lies within the range of the plot). Note also that the various curves are not continued below $z = 3$ (for $V_c = 285$ km/s) or $z = 6$ (for the other cases).

5 show the ratio $N_{1/2}$ in the approximate calculation, for \bar{x}^i ranging from 1 down to 10^{-9} , over the whole relevant range of source masses, i.e., assuming a minimum $V_c = 4.5, 16.5, 35, 80,$ or 285 km/s, and for four values of the efficiency ζ , 19, 95, 580, and 5800. It is interesting to consider the whole parameter space, without normalizing to a particular reionization redshift, since the dominant population of ionizing sources at any given redshift may not have similar properties to that near the end of reionization, due to the evolution in time of chemical, radiative, and hydrodynamical feedbacks.

The above values of ζ are chosen to be particularly interesting, where $\zeta = 19$ corresponds to $z_{\text{rei}} = 7$ for $V_c = 16.5$ km/s, and $\zeta = 95$ corresponds to $z_{\text{rei}} = 3$ for $V_c = 285$ km/s, which are the H and He reionization examples considered in the previous subsection. More generally for star-forming halos, Population II stars (assumed similar to low-metallicity stars forming today) produce ~ 5800 ionizing photons per hydrogen atom in stars, while Population III stars (assumed to consist of $100M_{\odot}$, zero-metallicity stars) produce around 10 times more. Thus, if we assume a maximum star formation efficiency of 10% (i.e., that this fraction of the baryons in a halo are contained in stars), then if all ionizing photons escape out of the dense surroundings of the stars and the halo, we get a maximum possible $\zeta = 5800$, with Pop III stars. A value of $\zeta = 580$ can then represent several possibil-

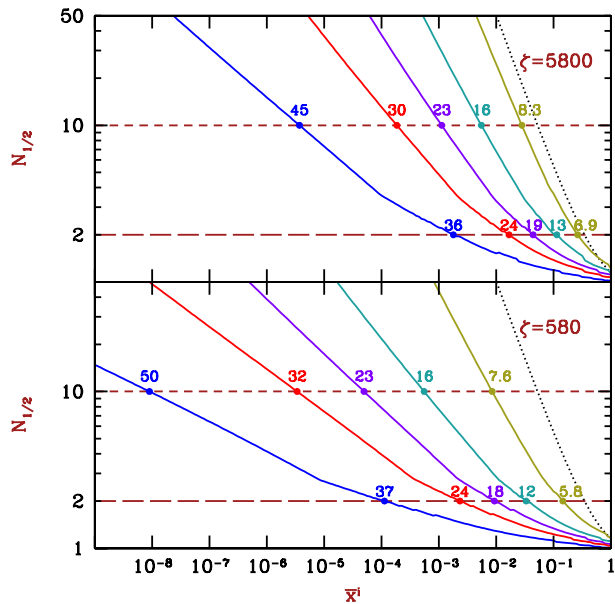


Figure 5. Same as Figure 4 but for $\zeta = 580$ or 5800 , as indicated.

ities: perhaps only 10% of photons escape, or 100% escape but we assume Pop II stars, or we assume Pop III stars but with a star formation efficiency of only 1%. The latter value is indeed the efficiency expected for the very first, primordial Pop III stars in molecular cooling halos. Numerical simulations suggest that in each $\sim 10^5 M_\odot$ halo (containing, therefore, $\sim 10^4 M_\odot$ in baryons), it is likely that only a single $100 M_\odot$ star forms (Yoshida et al. 2006) before its feedback disrupts the rest of the halo gas and prevents the formation of additional stars, at least for some time. Note also that these values of ζ neglect recombinations, which can only lower the effective ζ further.

Figures 4 and 5 imply the general conclusion that ionizing sources produce isolated, single-source bubbles only quite early in reionization, when $\bar{x}^i \ll 1$. This is a result of the fact that while Poisson fluctuations are large when we consider just one or two sources, they are strongly modulated by halo bias due to the underlying density fluctuations. Thus, sources are usually found in high-density regions, which makes it relatively likely to find other sources nearby. As sources become rarer at high redshift, the increasing correlation strength between halos partially compensates for the overall low number density of sources, though eventually the sheer rarity of sources does come to dominate. As discussed above, increasing V_c or ζ at a given \bar{x}^i makes sources rarer and brings larger scales into play, making it easier to form one-source bubbles relative to multi-source bubbles. However, only the most extreme case we consider of rare, extremely bright sources ($V_c = 285$ km/s and $\zeta = 5800$, an highly unlikely combination) approaches the results expected for a pure stochastic Poisson distribution; the ratio in the stochastic model is $N_{1/2} = 1/[1 - \exp(-2\bar{x}^i)]$ (Furlanetto & Oh 2008).

The Figures also indicate the redshifts when the fraction $F_i(N = 1)$ of the ionized volume that is contained in one-source bubbles equals 50% (corresponding to $N_{1/2} = 2$) or 90% ($N_{1/2} = 10$). In particular, for $V_c = 16.5$ km/s normal-

ized to produce H reionization at $z_{\text{rei}} = 7$ (i.e., $\zeta = 19$), one-source bubbles dominate (i.e., $F_i(N = 1) > 90\%$) only above $z = 57$ (outside the plot range), while multi-source bubbles become equally important (i.e., $F_i(N = 1) = 50\%$) at redshift 30. Primordial Pop III stars with $\zeta = 580$ and $V_c = 4.5$ km/s also tend to form multi-source bubbles at rather high redshifts, with one-source bubbles remaining dominant only down to $z = 50$, and with multi-source bubbles becoming equally important at $z = 37$. On the other hand, for He reionization at $z_{\text{rei}} = 3$ with $V_c = 285$ km/s (i.e., $\zeta = 95$), these milestones are reached at $z = 7.7$ and $z = 5.2$, respectively. Additional cases where these milestones occur outside the plot range of the Figures include $\zeta = 95$ and $V_c = 4.5$ km/s, which reaches $N_{1/2} = 10$ at $z = 62$; $\zeta = 19$ and $V_c = 35$ km/s, which reaches $N_{1/2} = 10$ at $z = 37$; and the faintest example we consider for individual sources, $\zeta = 19$ and $V_c = 4.5$ km/s, which reaches $N_{1/2} = 2$ at $z = 53$ and does not reach $N_{1/2} = 10$ even at the most likely redshift ($z = 65$) of the very first star (Naoz et al. 2006).

If we consider a range of values of ζ for halos of a given V_c , the global ionized fraction \bar{x}^i corresponding to a particular milestone (as defined by a particular value of $F_i(N = 1)$) increases with ζ , since increasing ζ at a fixed \bar{x}^i makes sources rarer, while increasing \bar{x}^i (with a fixed ζ) compensates for this by increasing the source number density. For each milestone, however, the redshift, which observationally is the most directly relevant quantity, behaves in a more complicated way, since it is directly related to the number density of sources, and thus depends on the ratio \bar{x}^i/ζ . We find that sources with a given V_c can only achieve a dominance of one-source bubbles at high redshift, almost regardless of the efficiency ζ (and thus, regardless of the reionization redshift).

Figure 6 shows the minimum z required to achieve various values of $F_i(N = 1)$ (as a function of V_c), assuming only that the value of ζ lies within some wide range. The figure shows that while high values of ζ do have a larger effect on low- V_c halos, the minimum redshift is overall relatively insensitive to the particular range assumed. In particular, assuming $10 < \zeta < 1000$, for He reionization by quasars (assuming $V_c \leq 300$ km/s), the volume fraction in one-source bubbles $F_i(N = 1)$ can be greater than 50% only at $z > 4.9$, 90% at $z > 7.3$, and 99% at $z > 9.1$. For H reionization by stars (assuming $V_c \leq 35$ km/s), these milestones require $z > 18$, $z > 23$, and $z > 28$, respectively. The generation of atomic-cooling halos ($V_c = 16.5$ km/s) can achieve $F_i(N = 1) > 50\%$ only at $z > 24$, 90% at $z > 31$, and 99% at $z > 38$. Finally (again assuming $10 < \zeta < 1000$), the earliest generation of molecular-hydrogen-cooling halos ($V_c = 4.5$ km/s) can achieve these milestones only at $z > 36$, $z > 48$, and $z > 61$, respectively.

3.3 Later stages

As reionization advances, eventually the typical bubble size encompasses a large number of ionizing sources, reducing the importance of discreteness and of Poisson fluctuations. Figures 7 and 8 show the cumulative bubble size distribution as in Figure 2, but for later stages of reionization. At these times, the continuous barrier models still have a significant probability at $V < V_{\text{bub}}$, especially for He reionization by quasars; however, if only the $V > V_{\text{bub}}$ portion is considered

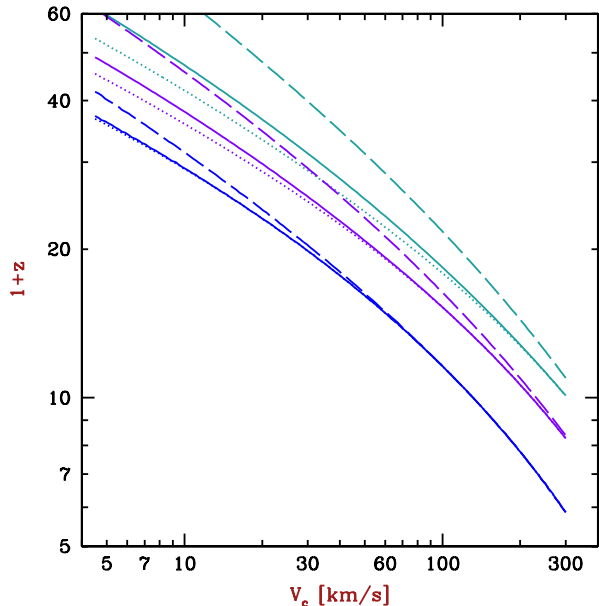


Figure 6. Minimum redshift (shown in terms of $1+z$) required to achieve a dominance of one-source bubbles, for ionizing sources in halos with a minimum circular velocity V_c (shown over the range 4.5 – 300 km/s). The minimum redshift shown here is required regardless of the reionization redshift or the ionizing efficiency, as long as ζ is in the range 10–100 (dashed curves), 10–1000 (solid curves), or 10–10000 (dotted curves). We consider milestones when the volume fraction in one-source bubbles is 50%, 90%, or 99% (from bottom to top in each set of curves).

as in these figures (see also the discussion in section 3.1), then the linear barrier predictions become essentially identical to those of the exact barrier, and the predicted bubble size distributions of these continuous models are reasonably accurate. Specifically, when $\bar{x}^i = 10\%$, for the example of H reionization, $V_{1/2}$ and $V_{1/100}$ equal 1.08 and 2.28, respectively, in model A (the full model), 1.06 and 2.18 in model B (continuous barrier), and 1.06 and 2.16 in model C (linear barrier). For He reionization, $V_{1/2}$ and $V_{1/5}$ are 1.42 and 2.56 in model A, 1.44 and 2.98 in model B, and 1.44 and 2.99 in model C. When the universe is 10% ionized, bubbles with a small number of sources still play a major role, e.g., one and two-source bubbles together account for 19% (H) or 60% (He) of the total ionized volume, and the small- N regime is still quite important.

At the midpoint of global reionization ($\bar{x}^i = 50\%$), the continuous barrier models approach the full model even more (note that the figures at different \bar{x}^i have different y -axis ranges). For the example of H reionization, $V_{1/2}$ and $V_{1/100}$ equal 1.03 and 1.22, respectively, in model A (the full model), 1.01 and 1.19 in model B (continuous barrier), and 1.01 and 1.19 in model C (linear barrier). For He reionization, $V_{1/2}$ and $V_{1/5}$ are 1.08 and 1.23 in model A, 1.08 and 1.24 in model B, and 1.08 and 1.24 in model C. For H reionization only 5.2% of the ionized volume lies in one and two-source bubbles, but for He this fraction is still 17%. As we found in section 3.1 at $\bar{x}^i = 1\%$, at $\bar{x}^i = 10\%$ and 50% we again see that the pure Press-Schechter model (Model D) is a rather poor approximation to model C, and that the pure

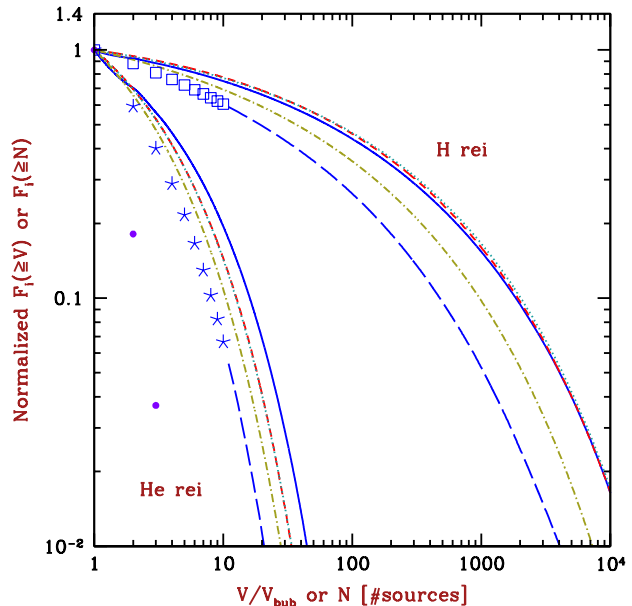


Figure 7. Cumulative bubble size distribution as a function of V/V_{bub} , or of the number N of ionizing sources in the bubble. Assuming $z_{\text{rei}} = 7$ and $V_c = 16.5$ km/s for H, and $z_{\text{rei}} = 3$ and $V_c = 285$ km/s for He, we consider $\bar{x}^i = 10\%$ ($z = 12.1$ for H, 4.8 for He). We compare $F_i(\geq V)$, the fraction of the ionized volume contained in bubbles with volume $\geq V$, between model A (solid curves), model B (short-dashed curves), model C (dotted curves), and model D (dot-dashed curves). We also show $F_i(\geq N)$, the fraction of the ionized volume contained in bubbles containing $\geq N$ sources, from model A (H: squares, He: stars; long-dashed curves for $N > 10$) and model E (circles). Note that the curves for models B and C essentially overlap.

Poisson model (Model E) predicts a distribution by number $F_i(\geq N)$ that falls off much faster with N than do the true distributions (for H or He reionization) according to model A.

4 CONCLUSIONS

We have developed a model of reionization that adds discrete ionizing sources and Poisson fluctuations to the continuous model of Furlanetto et al. (2004). We have shown how to obtain the distribution of ionized bubbles, versus both bubble size and number of ionizing sources, with a two-step Monte Carlo method that accounts for both density and Poisson correlations among regions of various sizes surrounding a given random point in the universe. The bubble size distribution we obtained differs substantially from previous models, but if the continuous barrier model is cut off below V_{bub} (the minimum bubble volume corresponding to a single halo of mass M_{min}) then it yields a reasonable rough estimate to the true bubble size distribution. More specifically, this estimate is generally accurate for H reionization even as early as a mean ionized fraction $\bar{x}^i = 1\%$, while for He reionization it works best for small volumes and at later times, and at $\bar{x}^i = 1\%$ is accurate only up to $V \sim 3V_{\text{bub}}$. Note that with the cutoff at V_{bub} , the linear barrier approximation (which

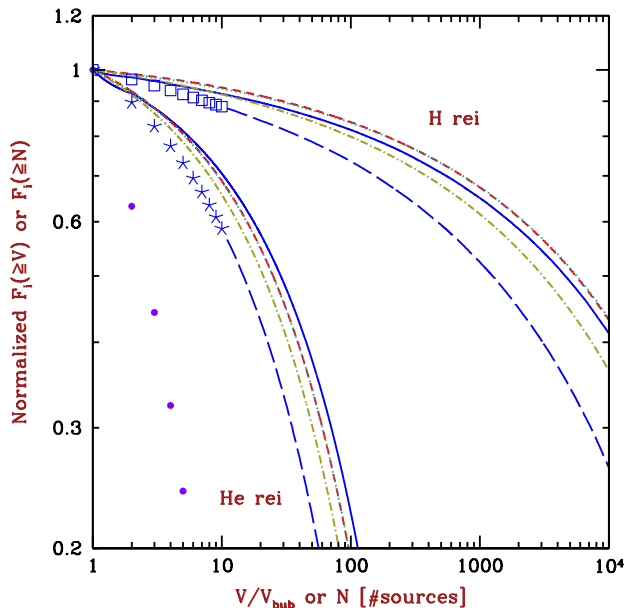


Figure 8. Cumulative bubble size distribution as a function of V/V_{bub} , or of the number N of ionizing sources in the bubble. Same as Figure 7, except calculated when $\bar{x}^i = 50\%$ ($z = 8.7$ for H, 3.6 for He). Note that the curves for models B and C essentially overlap.

can be calculated analytically) gives nearly identical results to the exact continuous barrier.

Our full model yields a bubble distribution by number N that drops more rapidly with N than does the volume distribution drop with V , but still, multi-source bubbles are always far more abundant than a pure stochastic Poisson model would suggest. This is due to the fact that density fluctuations are strongly correlated with ionization even when Poisson fluctuations are large. Thus, the density of ionized regions is strongly biased high compared to unconstrained regions, but on the other hand, Poisson fluctuations allow regions to fully ionize themselves even if their density is not as high as would be needed in the continuous barrier model.

The main parameters controlling the relative dominance of single-source bubbles are the effective efficiency ζ and the effective slope n of the power spectrum on the scale of a one-source bubble. The ratio of how much harder (in terms of number of σ of the fluctuation) it is to ionize large bubbles compared to small ones, is approximately proportional to $\zeta^{1+(n/3)} - 1$. Reionization by rare sources that are massive and bright corresponds to having a high ζ and to a high minimum bubble size, which brings larger scales into play, making the effective n less negative and thus making it harder to produce multi-source bubbles.

We have developed a quick, 15% accuracy approximate calculation of the ratio $N_{1/2}$ between the total ionized volume and that in multi-source bubbles. This allowed us to sweep through the full parameter space of possible halo masses and efficiencies of the ionizing sources, and to show that sources with a given minimum circular velocity V_c can only achieve a dominance of one-source bubbles at high redshift, regardless of their efficiency or of the reionization

redshift. In particular, for He reionization by quasars, one-source bubbles can dominate (i.e., contain 90% of the ionized volume) only at $z > 7.3$, and fill half the ionized volume at $z > 4.9$, while H reionization by stars can achieve these milestones only at $z > 23$ and $z > 18$, respectively (assuming $10 < \zeta < 1000$). The generation of atomic-cooling halos can place 90% of the ionized volume in isolated bubbles only at $z > 31$ and 50% at $z > 24$, while the earliest generation of molecular-hydrogen-cooling halos can achieve the same only at $z > 48$ and $z > 36$, respectively.

We note that reality likely includes even more fluctuations than included in our Poisson model, since we have still assumed that the number of ionizing photons emitted from a galactic halo is proportional to its mass. In reality, variations in the ionizing efficiency (through spatial or temporal fluctuations in the star formation efficiency and in the escape fraction of ionizing photons), and in the merger histories of halos of a given mass (even within a given environment, as measured by the average density of a surrounding region) will increase the role of (now generalized) Poisson fluctuations compared to that of galaxy bias due to the underlying large-scale density fluctuations. Simple forms of such variability can be included in a model of the type that we presented, since the ionizing photon outputs from sources are added as individual units (which could be generated from additional distributions for a given halo mass). In general, the model we developed can be used to investigate helium reionization and observational prospects for 21-cm observations during the infancy of hydrogen reionization.

ACKNOWLEDGMENTS

The author thanks Andrei Mesinger for very useful comments, and is grateful for support from the ICRR in Tokyo, Japan, the Moore Distinguished Scholar program at Caltech, and the John Simon Guggenheim Memorial Foundation, as well as Israel Science Foundation grant 629/05.

REFERENCES

- Barkana R., 2007, MNRAS, 376, 1784
- Barkana R., Loeb A., 2004, ApJ, 609, 474
- Barkana R., Loeb A., 2005a, ApJ, 624, L65
- Barkana R., Loeb A., 2005b, ApJ, 626, 1
- Barkana R., Loeb A., 2007, Rep. Prog. Phys., 70, 627
- Barkana R., Loeb A., 2008, MNRAS, 384, 1069
- Bond J. R., Cole S., Efstathiou G., Kaiser N., 1991, ApJ, 379, 440
- Cen R., 2006, ApJ, 648, 47
- Chuzhoy L., Alvarez M. A., Shapiro P. R., 2006, ApJ 648 L1
- Furlanetto S. R., McQuinn M., Hernquist L., 2006a, MNRAS, 365, 115
- Furlanetto S., Oh S. P., 2008, ApJ, 681, 1
- Furlanetto S. R., Oh S. P., Briggs, F., 2006b, Phys. Rep., 433, 181
- Furlanetto S. R., Zaldarriaga M., Hernquist L., 2004, ApJ, 613, 1
- Hogan C. J., Rees M. J., 1979, MNRAS, 188, 791

- Komatsu E., et al., 2008, ApJS, submitted (arXiv:0803.0547)
- Madau, P., Meiksin, A., Rees, M. J., 1997, ApJ, 475, 429
- Mellema, G., Iliev, I. T., Pen, U.-L., Shapiro, P. R. 2006, MNRAS, 372, 679
- Mesinger, A., & Furlanetto, S. 2007, ApJ, 669, 663
- Naoz, S., Barkana, R., 2008, MNRAS, 385, 63
- Naoz S., Noter S., Barkana, R., 2006, MNRAS, 373, L98
- Press W. H., Schechter P., 1974, ApJ, 187, 425
- Pritchard J. R., Furlanetto S. R., 2006, MNRAS 367, 1057
- Pritchard J. R., Furlanetto S. R., 2007 MNRAS 376, 1680
- Scott D., Rees M. J., 1990, MNRAS, 247, 510
- Sheth R. K., Tormen G., 1999, MNRAS, 308, 119
- Sheth R. K., Tormen G., 2002, MNRAS, 329, 61
- Trac H., Cen R., 2007, ApJ, 671, 1
- Yoshida N., Omukai K., Hernquist L., Abel T., 2006, ApJ, 652, 6
- Zahn O., Lidz A., McQuinn M., Dutta S., Hernquist L., Zaldarriaga M., Furlanetto S. R., 2007, ApJ, 654, 12
- Zhang J., Hui L., 2006, ApJ, 641, 641